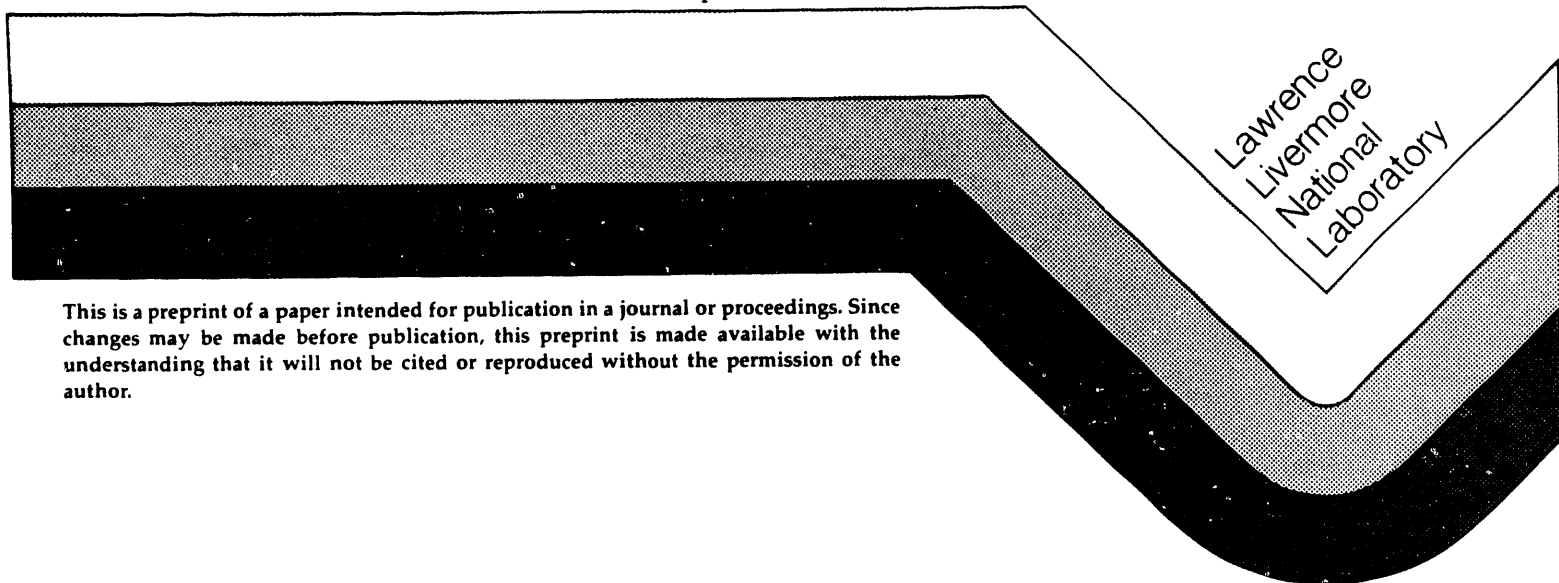Conf-910968--20

Rec...

OCT 2 5 1991

NUMERICAL SIMULATION OF THE STABILITY IN A CABLE-IN-CONDUIT CONDUCTOR DEVELOPED FOR FUSION-MAGNET APPLICATIONS

R.L. Wong, C.T. Yeaw, S.S. Shen, and J.R. Miller

This paper was prepared for submittal to
14th Symposium on Fusion Engineering
San Diego, CA
September 30 - October 3, 1991

September 25, 1991

Lawrence
Livermore
National
Laboratory

MASTER

DISTRIBUTION OF THIS DOCUMENT IS UNLIMITED

DISCLAIMER

NUMERICAL SIMULATION OF THE STABILITY IN A CABLE-IN-CONDUIT CONDUCTOR DEVELOPED FOR FUSION-MAGNET APPLICATIONS

R.L. Wong, C.T. Yeaw*, S.S. Shen, and J.R. Miller**
Lawrence Livermore National Laboratory
University of California
P.O. Box 5511, L-643
Livermore, California 94550
*University of Wisconsin
**National High Magnetic Field Laboratory, Florida State University

Abstract

The stability margins of the US-Demonstration Poloidal Coil (US-DPC) and the International Thermonuclear Experimental Reactor (ITER) TF coils have been modeled numerically using the computer program CICC. The computed US-DPC limiting current, I_{lim}, compares favorably with the values determined experimentally. Using the detailed program CICC output, we investigated the DPC quench initiation mechanism in each of the three stability regions. In the ill-cooled region, the imposed heat pulse heats the conductor to the current-sharing temperature, T_{cs}. In the transition region, the resistance heating after the pulse must be strong enough to overcome the induced flow reversal. In the well-cooled region, good heat transfer heats the helium during the pulse. After the pulse, these high helium temperatures along with poor heat transfer cause the conductor to quench. Changes in I_{lim} agree with Dresner's relationship. I_{lim} can be improved by decreasing the copper resistivity, the helium fraction, or the conductor diameter. Preliminary results show the ITER TF coil operating point is in the well-cooled region.

Introduction

Cable-in-conduit conductors (CICC) are gaining broader acceptance in cryogenic superconducting magnet designs. These conductors are made by twisting copper stabilized Nb_3Sn or NbTi superconductor wires into cables and enclosing them tightly in a conduit. Supercritical helium is forced through the interconnected spaces between the superconducting wires for cooling and stabilization.

An important consideration in the design of a CICC is the maximum energy pulse that the conductor can absorb and still retain (or recover) its superconducting operating state. The stability or energy margin has been determined experimentally for many CICCs. Definitive early experiments on model conductors were done by Lue, et.al.[1,2] Plots of the energy input to quench vs current typically display three stability regions: high stability at low currents; low stability at high currents; and a steep transition. The separation of the regions is understood in terms of differences in the heat transfer caused by induced flow. At low currents, strong energy pulses induce high helium velocities, and the conductor is said to be convectively well-cooled. At high currents weak energy pulses induce low helium velocities, and the conductor is said to be ill-cooled. The transition region can have a multivalued Z shape with three changes between stable and unstable behavior at a given current. The current at the intersection of the ill-cooled and transition regions is called the limiting current, I_{lim}, since it is desirable to limit

currents in a magnet design to less than I_{lim} and operate in the higher stability region.

This stability behavior has been predicted analytically. Dresner obtained a closed form solution for I_{lim} for conductors with initially stagnant helium by evaluating the convective heat-transfer coefficient from the thermal expansion of the helium.[3] The quench occurs at the time when the transient heat-transfer coefficient is minimum. Bottura, in his HESTAB code, expanded Dresner's work by including the effects of friction and forced flow.[4] Both analyses show agreement with experiments by Lue, et.al. near I_{lim}.[1,2] E. Tada, et.al solved the helium and conductor conservation equations by finite difference, obtaining agreement with their stability measurements.[5] The present work reports the use of a new numerical analysis tool, the CICC computer code, for the study of a recent coil test where fusion relevant CICCs were applied.[6] This code solves the conservation equations in the helium flow, conductor, and conduit.

Stability Analysis of the US-DPC

The US-DPC was built by the Massachusetts Institute of Technology and tested at the Japan Atomic Energy Research Institute in late 1990 as part of a cooperative fusion magnet development program.[7,8] DC testing to the 30 kA (5.66 T) operating current resulted in no problems. However the coil quenched unexpectedly during AC loss testing while attempting to reach 30 kA by ramping up in 1 s. To investigate this problem, the coil was tested to a range of currents by ramping up at increasing ramp rates until it quenched. All quenches occurred in pancake coil C. The significant difference between pancake C and the other pancakes is that it has a larger helium fraction because it is the only coil with no imbedded heater (the heater was not used). It is thought that AC eddy current heating losses are partially responsible for the quenches, since these losses increase with increasing ramp rate. The exact nature of the destabilizing heat pulse in the experiment has not been determined and is still under investigation. Possible sources are AC heating, magnetic flux jumping, mechanical work, or some combination. A plot of ramp rate vs current does have the general shape of a stability curve with I_{lim} in the range of 20–26 kA, suggesting that the destabilizing energy release is related to the ramp rate.[8] This initiated a detailed computational study into the stability behavior of the coil.

The cross-section of the US-DPC conductor is shown in Fig. 1. The basic CICC conductor geometry is modified in this instance by adding an outer conduit, providing an additional helium path between the two conduits. The stability curves, calculated over a range of possible US-DPC
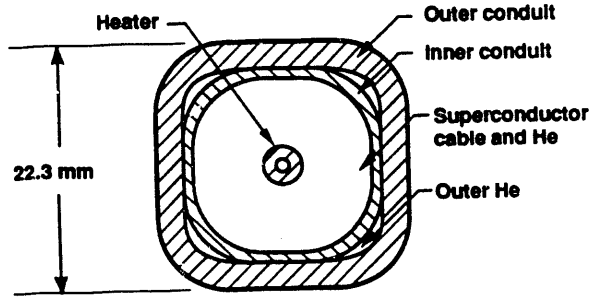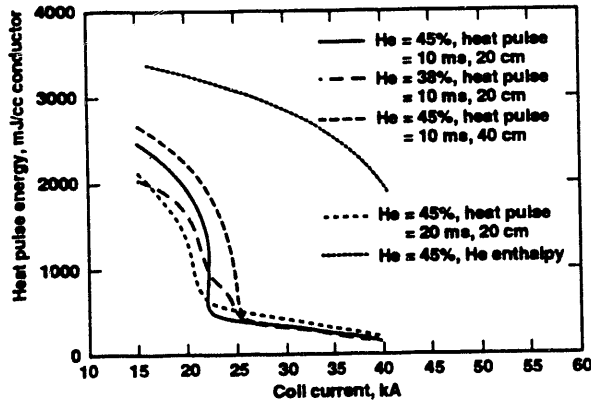
Figure 1. US-DPC Conductor Geometry
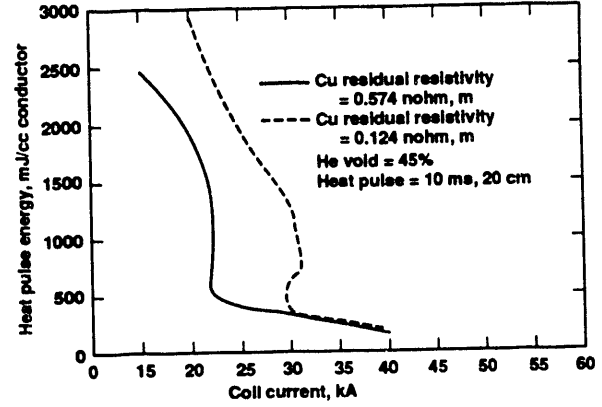

Figure 2. CICC Simulation of US-DPC

Figure 3. CICC Simulation of US-DPC Effect of Cu Resistivity

1/5 and 2/5 to 1/15 and 2/15.[9] The modified Dresner Equation is:

$$J_{lim} \propto \left[\frac{f_{Cu}(1-f_{co})}{f_{co}} \right]^{1/2} \left[\frac{(T_{cr}-T)^{1/2} \ell^{2/15}}{\rho^{1/2} D_h \tau^{1/15}} \right] \qquad (1a)$$

or

$$I_{lim} \propto \left[\frac{A_{Cu}A_{He}}{A_{co}} \right]^{1/2} \left[\frac{(T_{cr}-T)^{1/2} \ell^{2/15}}{\rho^{1/2} D_h \tau^{1/15}} \right] \qquad (1b)$$

where:

J_{lim} = Limiting current density in the conductor
= I_{lim}/A_{co}
A_{co} = Area of the conductor
A_{He} = Area of the helium
A_{Cu} = Area of the copper
f_{Cu} = Volume fraction of copper in the conductor
f_{co} = Volume fraction of conductor in the cable space
= $1-f_{He}$
T_{cr} = Critical temperature of the conductor
T = Helium temperature
ρ = Electrical resistivity of the copper
ρ_0 = Residual electrical resistivity of the copper
τ = Heat pulse duration
ℓ = Heated zone length
D_h = Hydraulic diameter

To first order, A_{He} enters into the conservation equations only through the hydraulic diameter,

$$D_h = \frac{4 A_{He}}{P} \qquad (2)$$

where P is the heat-transfer perimeter. Also to first order, D_h can be expressed in terms of f_{He} and the wire diameter, d, by

$$D_h = \frac{f_{He}}{1-f_{He}} d \qquad (3)$$

parameters are shown in Fig. 2. The helium enters at 4.5 K and 0.6 MPa, and exits at 0.5 MPa. Since the outer helium flow provides a heat sink, a constant temperature 4.5 K boundary condition is used outside the inner conduit. The calculations show that only 10% of the generated heat is removed by this outer helium flow during the first 0.1 s after heat pulse initiation, when stability is determined. Helium in the outer flow path contributes little to the stability of the conductor but may be useful for steady heat removal. In the simulation, the square heat pulse is imposed at the middle of the inner coil turn where the magnetic field is highest and a quench is most likely to occur. The parameters chosen for the different stability curves are: helium fraction, f_{He} (representing conditions with and without the heater), heat pulse duration, τ, and heated zone length, ℓ. The choice of τ and ℓ reflect uncertainties regarding the nature of the heat pulse. The stability curves show that the US-DPC performance is not totally unexpected. There is a clearly limiting current in the range of 21–26 kA. The quenches occur in pancake C, since the I_{lim} is lower due to the greater f_{He}. A significant contributor to the depressed I_{lim} is the poor conductivity of the copper stabilizer. The effect of changing the stabilizer resistivity, ρ, is investigated in Fig. 3. These curves show that if a copper is used that has 4.63 times less residual resistivity, ρ_0, (i.e. the copper used in the ITER design) I_{lim} is increased by 8 kA.

Dresner's equation predicts how I_{lim} should vary with changes in conductor and heat pulse parameters.[3] Based on experimental data, Miller and Lue changed the exponents of τ and ℓ, respectively, from

I_{lim} can be increased by either decreasing the void fraction or the wire diameter. The decrease in f_{He} from 45% to 38% was accomplished by changing A_{He}. If Eqn. (1a) is combined with Eqn. (2), the effect of A_{He} on I_{lim} becomes:

$$I_{lim} \propto \frac{1}{(A_{He})^{1/2}} \tag{4}$$

The change in I_{lim} as calculated by Eqn. (1a) and as read from the stability curves in Figs. 2 and 3 for the different curve parameters is shown in Table 1. The reference case is $f_{He} = 45\%$, $\tau = 10$ ms, $\ell = 20$ cm. Table 1 lists the I_{lim} ratio resulting from each curve parameter ratio (with respect to the reference case).

Table 1. US-DPC Limiting-Current-Ratio Comparison

Parameter	Parameter	Dresner	CICC Code Calculation
	$Parm/Parm_{ref}$	$I_{lim}/I_{lim\ ref}$	$I_{lim}/I_{lim\ ref}$
Hydraulic Dia., $A_{He}/A_{He\ ref}$	0.748	1.156	1.146
Heating Duration, τ/τ_{ref}	2.0	0.955	0.963
Heated Length, ℓ/ℓ_{ref}	2.0	1.097	1.146
Copper Resistivity, $\rho_0/\rho_{0\ ref}$	0.216	2.152	1.352

The calculated changes for τ, ℓ, and A_{He} show good agreement with Eqn. (1). This verifies the validity of the change to the smaller exponents for τ and ℓ. The calculated change for ρ is somewhat less than given in Eqn. (1) due to the increasing field with increasing I_{lim}, which affects both T_{cs} and ρ.

Detailed output from the computational model allows insights into the thermo-fluid mechanisms that determine a quench initiation. Each of the three stability regions is characterized by its own specific mechanisms, but some general comments can be made. The heat pulse is imposed in the middle of the first or inlet turn, which is only 1.637 m long. The 0.1 MPa pressure drop (with 45% void) results in a steady state flow of 60.1 kg/s-m² (5.51 g/s). The inlet end of the coil is close enough for the heat pulse to cause a flow reversal, with helium discharging from the inlet. This is an important cooling mechanism since the initial transient conduction decays, and the heat transfer becomes dominated by forced convection after about 10 ms. The timing of the minimum heat-transfer coefficient, which occurs when the helium flow is near zero, determines the location of the quench initiation. With these general comments in mind, consider the mechanisms in each of the three stability regions.

In the low stability, ill-cooled region (currents greater than I_{lim} in Fig. 2), the stability mechanism is simple. A marginal quench is initiated when the heat pulse is strong enough to heat the conductor to T_{cs} at the end of the pulse (as assumed by Dresner). This occurs at a location near the middle of the heated zone, where the heat-transfer coefficient is minimum and the flow is near zero at the end of the pulse. Because the flow is near zero, there are significant conduction and laminar flow contributions; and

the Dittus-Boelter turbulent flow contribution is less than that assumed by Dresner. This is why the valid exponents of τ and ℓ are smaller.[9] When a quench is initiated in this region, the pulse heating rate is always equal to or less than the electrical resistance heating rate. After the pulse, the induced velocities are too low to recover the quench. This is why the region is termed ill-cooled. At I_{lim}, the pulse heating rate equals the electrical resistance heating rate. Figs. 4, 5, and 6 are transient profiles at the location of quench, just downstream of the middle of the heated zone, for a marginal quench near I_{lim}. The current is 22 kA and the 10 ms heat pulse has a strength of 575 mJ/cc (the lowest heat pulse in the multiple stability at 22 kA). Fig. 4 shows the heating rate where the quench initiated. The pulse heating rate and the resistance heating rate are nearly equal. A narrow heating spike at the end of the heat pulse is caused by resistance heating, but is too short to induce significant velocity. Fig. 5 shows how the transient heat transfer becomes dominated by convection after 10 ms. Fig. 6 shows the flow reversal resulting in zero velocity near the end of the heat pulse. In Fig. 2, the decrease in stability with increasing current in the ill-cooled region is the result of the increasing magnetic field and resulting decreasing T_{cs}. The only parameter having a significant influence on the energy margin in this region is the pulse
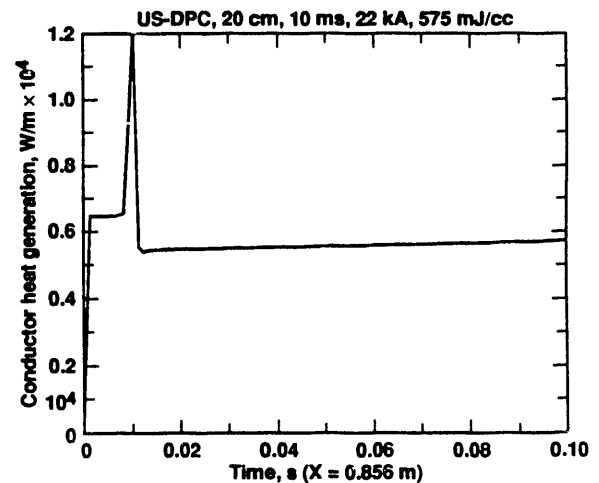

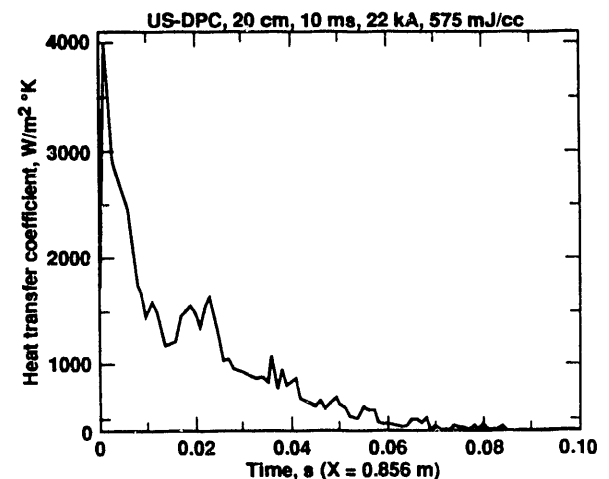Figure 4. Heating Rate During Quench Initiation

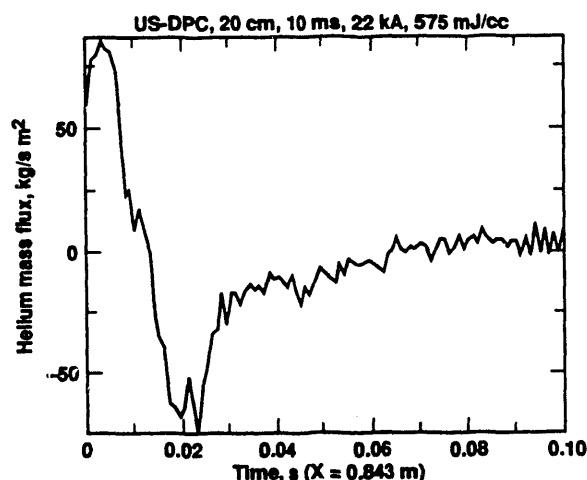Figure 5. Heat-Transfer Coefficient During Quench Near I_{lim}

Figure 6. Mass Flux During Quench Near I_{lim}

duration. Increasing the pulse duration lowers the pulse heating rate. This lowers the conductor-to-helium temperature difference more than the heat-transfer coefficient, producing a higher energy margin.

The key component of the transition region mechanism is a strong flow reversal after the pulse. This provides the high heat transfer necessary to recover a quench. To create this flow reversal, the heating rate during the pulse must be greater than the resistance heating rate. This causes a step decrease in heating. In the transition region, not only is the pulse heating rate higher, but the resistance spike at the end of the pulse is longer than it is at I_{lim}. The increased convection from the higher energy pulse and the lengthening resistance heating spike is reflected in the steepness of the transition region. At 22 kA, the increase in cooling capability is sufficient to create a multiple stability. The top of the transition region is typified by the resistance heating spike spreading over the entire heat-pulse duration. The quench initiates just downstream of the middle of the heated zone, where the flow is near zero at the end of the pulse. In Figs. 2 and 3, the changes in the transition region stability curve reflect the changes in I_{lim}.

At currents below 20 kA in the well cooled region, the quench mechanism changes. Quench initiation shifts from near the middle of the heated zone to the downstream end. This change is due to the significant heating of the helium. Initially the induced velocities and heat transfer coefficients are high, allowing the high heat pulse to heat the helium. Then the flow decays to near zero, producing low heat transfer coefficients, allowing the resistance heating to heat the conductor. "Well-cooled" does not mean that the helium and conductor temperatures are the same. Temperature differences of 7 K and 4 K during and after the pulse are typical. This quench mechanism at the end of the heated zone allows a smaller energy margin than does the mechanism in the transition region near the middle of the heated zone. Therefore the stability curve levels off in the well-cooled region (Fig. 2). Decreasing the helium fraction decreases the stability in the well-cooled region, since less helium heat capacity is available. Note in Fig. 2 that the 45% and 38% helium curves cross between I_{lim} and the well-cooled region. Decreasing the helium

fraction is beneficial in the transition region near I_{lim}, but is detrimental in the well-cooled region. Increasing the heated length increases the stability due to the greater velocities and heat-transfer coefficients during the pulse. During the 10-ms pulse duration, the helium travels only 4 cm so the additional heat added to the helium by increasing the heated length from 20 cm to 40 cm increases the helium temperature only slightly. Increasing the pulse duration decreases the stability in the well-cooled region due to the lower velocities and heat-transfer coefficients during the pulse. Again the stability curves cross, reflecting the opposite effects in the well-cooled and ill-cooled regions. A decrease in the copper ρ_0 results in increased stability throughout the well-cooled region due to the lower resistance heating..

Stability Analysis of the ITER TF Coil

Fig. 7 is a stability curve calculated for the ITER TF coil.[10] In contrast to the US-DPC curves, the ITER curve is almost a straight line with no definable separate stability regions. The coil has ten turns of CICC, each 40 m long, When the operating cycle temperatures are maximum, the quench is initiated in the middle of the inlet first turn with a 10-ms, 2-m pulse. The helium at the inlet is at 4.5 K and 0.65 MPa. The outlet is at 0.35 MPa. The 39m long ITER TF inlet turn is 24 times longer than the US-DPC inlet turn, so the TF quench does not see the end of the coil during the 0.1 s required for the determination of stability. The quench is symmetrical, flow reversal occurs just after the imposition of the heat pulse and has little effect on the quench. Even though there is no flow reversal at the end of the pulse, the induced outflow provides good convection cooling. Also the flow does not remain stagnant at the middle of the heated zone. Sonic pressure pulses initiated by the heat pulse generate velocities waves with maximum velocities of 0.5 m/s. Due to the long heated zone and the low T_{cs}, quench initiation is by the well-cooled mechanism except at the high-current end of the curve. The transition and ill-cooled regions are almost nonexistent. The ITER TF stability curve is below the US-DPC curve due to the higher TF field (lower T_{cs}). The TF design point is 37.9 kA (62.0 MA/m² cable space) with 11.2 T while the US-DPC operating point is 30 kA (147 MA/m² cable space) with
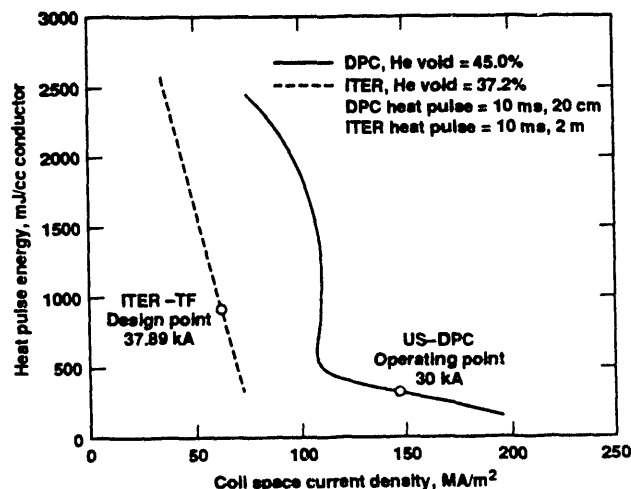

Figure 7. CICC Simulation of US-DPC and ITER-TF

5.66 T. The ITER TF operating point has a good energy margin of 925 mJ/cc. Further studies of the ITER quench phenomena are planned in the future, particularly with shorter heated zones.

Conclusions

The CICC computer code predicts stability curves for the US-DPC that agree with the experimental I_{lim}. An analysis of the computed thermo-fluid parameters in the three stability regions shows that:

1. In the ill-cooled region a quench is initiated when the heat pulse heats the conductor to T_{cs} at the end of the pulse. It occurs near the middle of the heated zone where the flow is near zero at the end of the pulse. The the heat pulse heating rate is always equal to or less than the electrical resistance heating rate. At I_{lim} the heating rates are equal. Decreasing the resistivity of the copper, the helium fraction or the wire diameter increases I_{lim}.

2. In the transition region, as in the ill-cooled region, the quench initiates near the middle of the heated zone where the flow is zero at the end of the pulse. For the quench to continue it must be strong enough to overcome the cooling flow reversal. This flow reversal is initiated by the step decrease from the heat pulse heating rate to the electrical resistance heating rate.

3. In the well-cooled region, helium heating is significant. The quench initiates at the downstream end of the heated zone where the flow is high during the pulse and near zero shortly after the pulse. The good heat transfer during the pulse heats the helium. After the pulse the poor heat transfer and the high helium temperatures allow the resistance heating to quench the conductor.

Preliminary studies into the stability of the ITER TF coil indicates the coil operates in the well cooled stability region except at currents above the 37.9-kA design current. At the design point, energy margin is 925 mJ/cc.

CICC conductor stability is a complex phenomenon that generally requires numerically solving the helium and solid conservation equations. Simplifying approximations can be made the ill-cooled region where the quench initiation mechanism is simple.

References

[1]   J. W. Lue, J. R. Miller, and L. Dresner, "Stability of Cable-in-Conduit Superconductors," in J. Appl. Phys, vol. 51, no. 1, pp.772–783, Jan. 1980.

[2]   J. W. Lue and J. R. Miller, "Parametric Study of the Stability Margins of Cable-in-Conduit Superconductor: Experiment," in IEEE Trans. on Magnetics, vol. MAG-17, no. 1, pp.757–760, Jan. 1981.

[3]   L. Dresner, "Parametric Study of the Stability Margin of Cable-in-Conduit Superconductor: Theory," in IEEE Trans. on Magnetics, vol. MAG-17, no. 1, pp.753–756, Jan. 1981.

[4]   L. Bottura and J. V. Minervini, "Modelling of Dual Stability in a Cable-in-Conduit Conductor," in IEEE Trans. on Magnetics, vol. 27, no. 2, pp.1900–1903, March 1991.

[5]   E. Tada, et.al., "Downstream Effect on Stability in Cable-in-Conduit Superconductor," in Cryogenics, vol. 29, pp.830–840, Aug. 1989.

[6]   R. L. Wong, "Program CICC, Flow and Heat Transfer in Cable-in-Conduit Conductors," in Proc. of IEEE 13th Symp. on Fusion Engineering, vol. 2, 1989, pp. 1134–1137.

[7]   M. M. Steeves, et.al., "The US Demonstration Poloidal Coil," in IEEE Trans. on Magnetics, vol. 27, no. 2, pp. 2369–2372, March 1991.

[8]   M. M. Steeves, et.al., "Test Results from the Nb3Sn US-Demonstration Poloidal Coil," 12th Conf. on Magnet Tech., June 1991.

[9]   J. R. Miller and J. W. Lue, "Designing Internally Cooled Superconductors for Use in Large Magnets." in Proc. Stability of Superconductors in Helium I and Helium II, Saclay (France), International Institute of Refrigeration Paris, pp. 247–253, Nov. 16–19 1981.

[10]   J.Miller, ed., Report of Work by the Magnet Design Unit, ITER-EL-MG-1-9-3, LLNL-ITER-89-048, Lawrence Livermore Laboratory, June–Oct. 1989.

END

DATE FILMED

11/25/91